Effect of near and far-field earthquakes on RC bridge with and without damper

Omid Karimzade Soureshjani[a] and Ali Massumi*

Department of Civil Engineering, Faculty of Engineering, Kharazmi University, Tehran, Iran

Abstract.   This paper presents a study on the behavior of an RC bridge under near-field and far-field ground motions. For this purpose, a dynamic nonlinear finite element time history analysis has been conducted. The near-field and far-field records are chosen pairwise from the same events which are fits to the seismic design of the bridge. In order to perform an accurate seismic evaluation, the model has been analyzed under two vertical and horizontal components of ground motions. Parameters of relative displacement, residual displacement, and maximum plastic strain have been considered and compared in terms of near-field and far-field ground motions. In the following, in order to decrease the undesirable effects of near-field ground motions, a viscous damper is suggested and its effects have been studied. In this case, the results show that the near-field ground motions increase maximum relative and residual displacement respectively up to three and twice times. Significant seismic improvements were achieved by using viscous dampers on the bridge model. Somehow under the considered near-field ground motion, parameters of residual and relative displacement decrease dramatically even less than the model without damper under the far-field record of the same ground motion.

Keywords: near-field and far-field; seismic behavior of RC bridge; nonlinear time history analysis; viscous damper

1. Introduction

The characteristic behavior of structures under near-field ground motions can be different from those experience far-field ground motions (Davoodi and Sadjadi 2015). It is clear that the near-field ground motions have impulsive nature and this feature causes severe damages to structural systems chiefly at the base where the lateral forces are maximum (Massumi *et al*. 2017). In the last decade, the difference of seismic behavior of structures under the near-field ground motions in comparison with the far-field ground motions attracts the attention of many researchers. This issue becomes even more important when the effects of near-field ground motions have not considered in many seismic design codes directly. These effects have to consider and develop appropriately in seismic codes and provisions. The behavior of structures under earthquakes is largely related to the dynamic characteristics of the structure, earthquake and the site conditions. So, the features of earthquakes in the proximity of a fault system is completely different from remote fault systems (Stewart *et al*. 2002). There is no clear distance definition over which fault system may be classified as near-field or far-field but in general earthquake records with less than 15 km distance are considered as near-field earthquakes and more than 20 km are considered as far-field one (Davoodi *et al*. 2012). Recent seismic studies show that the ratio of maximum

vertical earthquake acceleration to maximum horizontal earthquake acceleration may be greater in near-field earthquakes compared to far-field earthquakes (Hoshikuma *et al*. 2011). The effect of near-field ground motions on seismic demand of RC buildings previously conducted by Massumi *et al*. (2019). The characteristics of a ground motion depend on parameters such as sit soil type, rupture system, and source to site distance and so on. So, specifications of a near-field ground motion are significantly different from a far-field ground motion. Near-field earthquakes generally have higher accelerations and higher frequencies amplitude (different frequency content) than far-field earthquakes and in addition, the near-field records may accompany with short-duration impulsive records at the beginning which is more obvious in displacement time history of the ground motion and finally more kinetic energy (Fig. 1). Also, near-field ground motions release significant energy in a short duration. These features of near-field ground motions require more attention than far-field records in the design of structures (Somerville *et al*. 1997, Bolt 1993, Bertero *et al*. 1978). These records (near-field) often include some (one or more) separate pulses in the acceleration, velocity and displacement time history (Corigliano 2007). However, a structure may resist under a far-field ground motion but they may suffer a lot of damage in structural elements or even collapse under near-field ground motions. Bridges are an essential part of the transportation system, any disturbance in the performance of the bridge can disable the transportation system (Sheikh *et al*. 2012). So, the investigation of the seismic behavior of bridges under near-field ground motions is more important than residential structures. In many important bridge design codes, (for example, Japan bridge design code and AASHTO), bridges are classified according to their importance levels. Based on the Japan bridge design code,

---

∗Corresponding author, Professor
  E-mail: massumi@khu.ac.ir
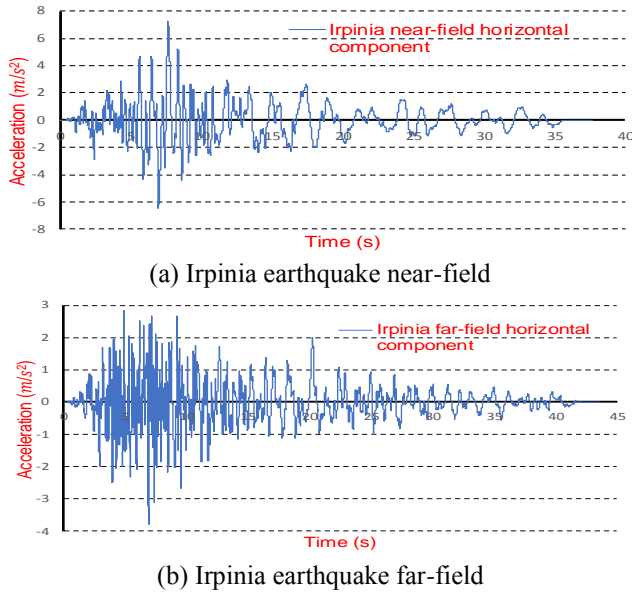[a]Ph.D. Student
  E-mail: std_omid.karimzade@khu.ac.ir

(a) Irpinia earthquake near-field

(b) Irpinia earthquake far-field

Fig. 1 Acceleration records of Irpinia earthquake

Table 1 Classification of bridges (Nihon Doro *et al* 1998)

Bridge Type	Definition
Type A	Bridges other than Type B bridges
Type B	• Bridges of National expressways, urban expressways, designated city expressways, and general national highways. • Double-deck bridges and over bridges of prefectural highways and municipal roads, and other bridges, highway viaducts, etc., especially important in view of regional disaster prevention plans, traffic strategy, etc.

Table 2 Primary and secondary loads for seismic design (Nihon Doro *et al*. 1998)

Primary loads	Secondary loads
Dead load Prestress force Effect of creep of concrete Effect of drying shrinkage of concrete Earth pressure Hydraulic pressure Buoyancy or uplift	Effects of earthquake

the studied bridge model in this paper is classified as Type B.

Past earthquakes show several problems in the seismic design and behavior of bridges. Bridges which have been designed based on old design codes show limited nonlinear behavior and energy dissipation under powerful ground motions. Some improvements in both analytical methods like ductility and performance have been achieved (the bridge design codes from 1990 have been fully updated) but the behavior of the bridges which even designed based on the new seismic design codes have not been directly evaluated (Nihon Doro 2002). During these years several studies have been done on the behavior of the structures under near-field earthquakes but major of them are limited to models of single degree of freedom (SDOF) or two-dimensional frame models under one component of ground motions. This article discusses the seismic behavior of a 3D RC single-span bridge under 3 different near-field and far-field ground motion acceleration records in two vertical and horizontal components. In order to decrease undesirable effects of near-field ground motions, a plan based on the viscous damper is suggested and its results have been studied. The analysis method is the dynamic implicit nonlinear time history finite element (FE) analysis. Parameters that have been measured and compared with each other in both cases of near and far-field ground motions are maximum displacement, maximum residual displacement, and maximum plastic strain. The type of the site soil and selected acceleration records match together. Near-field and far-field records are chosen pairwise from the same events. The outputs of this paper can be effective in summoning on the effect of near-field ground motions on bridges and considering their effects on future design codes.

2. Bridge model specifications

In seismic design, a bridge must be designed so that the seismic performance satisfies during an intended earthquake. The seismic performance of a bridge is determined by the importance of the bridge and also the levels of design ground motion that is likely to occur at the site of construction. Furthermore, the topographical, geological and site conditions must be considered in seismic design. The target bridge in this study is a bridge that has been designed based on the Japanese Design Specifications (it was designed based on nonlinear static analysis 1990). The bridge is a one span continuous girder bridge with a span length of 21.87 m and total deck length of 43.74 m, the bents supported eight steel beams, a concrete deck spanning between the two bents and the bents were composed of three columns which are indicated in Fig. 2. According to Table 1 the bridge model is classified as Type B. The deck on the columns axis has no expansion joints. Rigid elements are used to connect the deck and columns.

The design loads are divided into two main groups of primary and secondary loads. These loads are shown in Table 2. The load combinations should be: primary loads + earthquake loads which should be created the most critical condition (Nihon Doro *et al*. 1998).

RC bridge columns are designed to satisfy the Eqs. (1)-(3) which presented by Nihon Doro *et al*. (1998)

$$P_a \geq K_{hc} \times W \qquad (1)$$

$$W = W_u + c_p \times W_p \qquad (2)$$

where:

P_a: The lateral capacity of column,
K_{hc}: The design horizontal seismic coefficient,
W: The equivalent weight,
W_u: The weight of part of the superstructure,
W_p: The weight of the column,
c_p: The equivalent weight coefficient

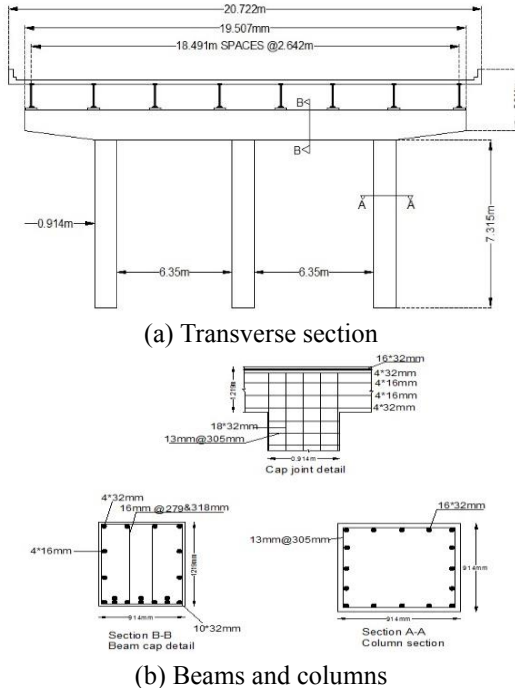The design horizontal seismic coefficient is calculated by using Eq. (3):

(a) Transverse section

(b) Beams and columns

Fig. 2 Details of the target bridge

Fig. 3 The FE bridge model

Fig. 4 Behavior diagram of concrete in compression

$$K_{hc} = c_s \times c_z \times K_{hc0} \geq 0.4 c_z \qquad (3)$$

where:

c_s: The response modification factor,

c_z: The zone modification factor (0.7, 0.85, or 1.0 depends on the site),

K_{hc0}: The standard modification coefficient

3. Theoretical basis of FEM analysis

The Abaqus software is used for analysis in this study which is a powerful FE analysis program to considering nonlinear behavior of materials. In this study by considering the nature of acceleration records and in order to accuracy, a nonlinear dynamic implicit FE method (FEM) with full Newton-Raphson solution analysis was used. The nonlinear dynamic analysis is achieved by direct time integration in degrees of freedom of the FE model. Abaqus implicit uses the Hilber-Hughes-Taylor (HHT) time integration by default (Abaqus Tutorial 2010). The HHT method is an extension of the Newmark-β method which is an implicit time integration. The main advantage of these time integration methods is that they are unconditionally stable for linear systems. Somehow this feature can be generalized to nonlinear analysis (Hilber *et al*. 1977). The HHT method can be defined based on the "half-increment residual" by using Eqs. (4)-(6) which has been introduced by Hibbitt and Karlsson (1979). So, at any time step for any degree of freedom

$$\Delta U|\tau = \tau^3 \Delta U|_{t+\Delta t} + \tau(1-\tau^2)\Delta t \dot{U}|_t + \tau^2(1-\tau)\frac{\Delta t^2}{2}\ddot{U}|t \quad (4)$$

$$\dot{U}|_t = \frac{\gamma}{\beta\tau\Delta t}\Delta U|\tau + \left(1-\frac{\gamma}{\beta}\right)\dot{U}|_t + \left(1-\frac{\gamma}{2\beta}\right)\tau \Delta t \ddot{U}|t \quad (5)$$
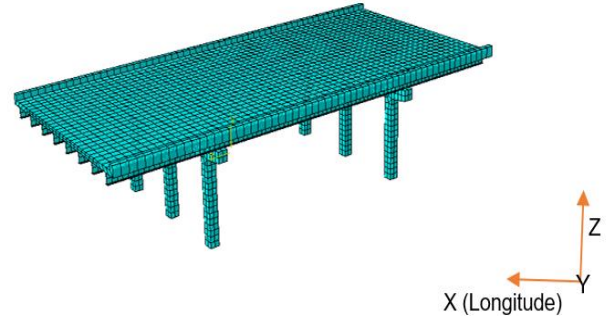
$$\ddot{U}|\tau = \frac{1}{\beta\tau^2\Delta t^2}\Delta U|\tau - \frac{1}{\beta\tau\Delta t}\dot{U}|_t + (1-\frac{1}{2\beta})\ddot{U}|t \qquad (6)$$

where:

$\ddot{U}$: The acceleration,

$\dot{U}$: The velocity,

U: The displacement,

$\Delta U|_{t+\Delta t} = U|_{t+\Delta t} - U|_t$,

$\beta = \frac{1}{4}(1-\alpha)^2$,

$\gamma = \frac{1}{2} - \alpha$

$-\frac{1}{2} \leq \alpha \leq 0$.

$0 \leq \tau \leq 1$

4. Methodology

4.1 Analytical model

The bridge has been modeled as a 3D model in Abaqus software. The analytical model has been shown in Fig. 3.

The bridge deck mass was modeled as continuous (close to the real condition of the bridge model). The concrete confinement has considered by using the transverse reinforcement as it has been previously shown in Fig. 2. The compressive strength of concrete is 25 MPa and the concrete damaged plasticity model has been chosen for modeling the property of the concrete materials which can be used for the behavior of concrete in the elastic-plastic form (in both types of compression and tensile). The stress-strain behavior of concrete (Figs. 4-5) has been calculated based on the numerical method which has been presented by HSU (1994).
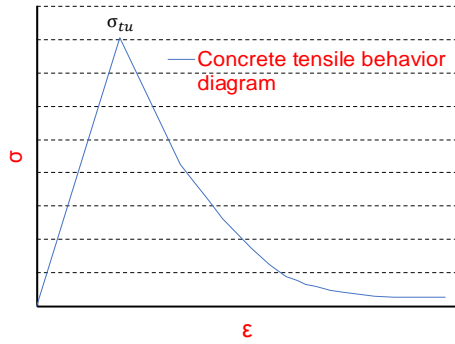
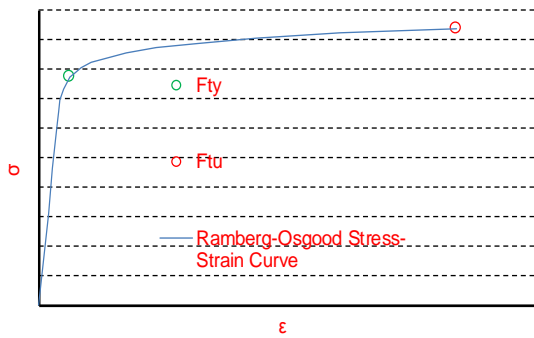Fig. 5 Behavior diagram of concrete in tensile

Fig. 6 Stress-strain curve for steel materials

The yield and ultimate strength of rebars which have been used in this model are 390 MPa and 570MPa respectively. The stress-strain behavior of rebars has been defined based on Ramberg and Osgood (1943) relationship by using Eq. (7). This relationship is useful for metals that harden with plastic deformation (like rebars). The calculated stress-strain diagram of steel has been shown in Fig. 6.

$$\varepsilon = \frac{\sigma}{E} + K\left(\frac{\sigma}{E}\right)^n \qquad (7)$$

The first term on the right side $\left(\frac{\sigma}{E}\right)$ is equal to the elastic part of the strain, while the second term $\left(K\left(\frac{\sigma}{E}\right)^n\right)$ accounts for the plastic part.
where:
ε: The strain,
σ: The stress,
E: The young modules,
K and n: The constants that depend on the material being considered.

4.2 Model verification

The verification of this study is based on a pushover analysis of a single degree of freedom (SDOF) column model which is conducted by Zhang *et al.* (2012). The intended model has shown in Fig. 7. The model is a SDOF column with section size of 6.5×6.5cm, the height of 260cm and the shear-span ratio is 4. Compressive strength of concrete is 21.2 MPa and longitudinal rebars yield and ultimate strength are 360 MPa and 540 MPa, respectively; transverse rebars (shear rebars) yield strength is 300 MPa; there is a lumped mass at the

(a) column model

(b) cross-section and reinforcement details
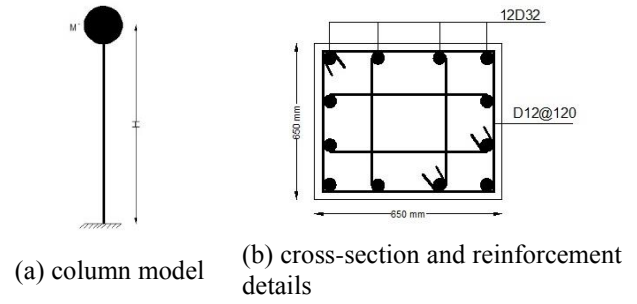
Fig. 7 Details of Zhang *et al.* model
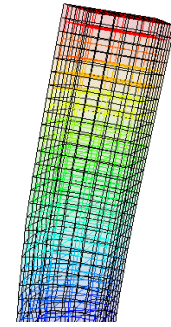
(a) FE model
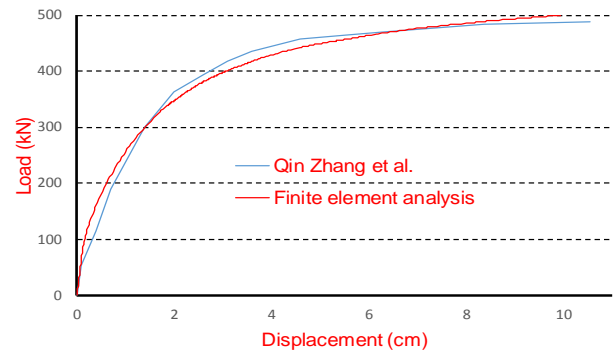
(b) Load-Displacement comparison

Fig. 8 Verification

Table 3 Comparison between FE analysis model and Zhang *et al.* (2012) model

Model	Load (kN)	Displacement (cm)
Qin Zhang *et al.*	359	1.76
FE model	359	1.84

top of the model (10e+5 kg) and the axial load is 1000 kN.

By comparing the results of Table 2 and Fig. 8, there is a little difference between the results of Zhang et. al (2012) model and FE analysis model (under 5%). Therefore, the FE results are valid.

4.3 Optimization analysis

To check the accuracy of the increment size and number of mesh (mesh size) that are chosen for the time history analysis of the bridge model, a convergence study was conducted.

4.3.1 Increment size optimization
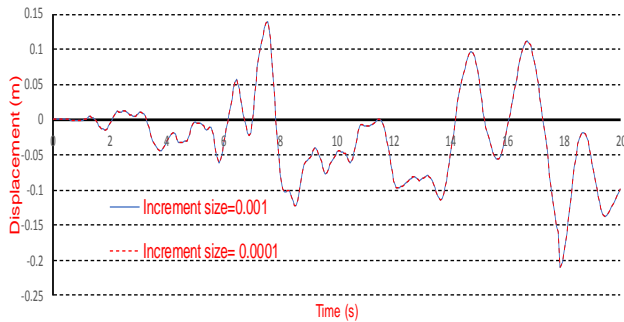The nonlinear implicit numerical time integration with the

Fig. 9 Time-history displacement of bridge deck with two different incremental sizes of 0.001 and 0.0001

Table 4 Maximum deck displacement with two different increment sizes

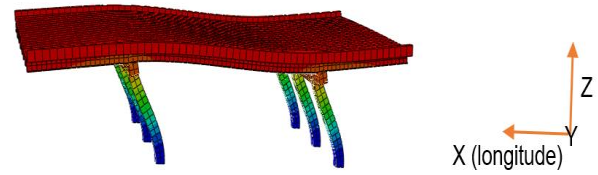| Incremental size	Maximum deck displacement (m)
0.001	0.2101
0.0001	0.2105

Fig. 10 First mode shape of the model with the frequency of 1.32 Hz and in longitude direction

Table 5 The natural period of bridge model with different size of the mesh

Total number of mesh	Natural Period (s)	Frequency (Hz)
22860	0.75	1.32
13989	0.75	1.32
13740	0.75	1.33
11612	0.75	1.33
7900	0.75	1.33
7224	1.11	0.91
6780	1.25	0.80

full Newton-Raphson method, the choice of increment size has a direct effect on the accuracy and computing cost (Cook 2007).

Results of the increment size of 0.001 were compared with the results of the increment size of 0.0001. The incremental sizes of 0.001 and 0.0001 were considered as accurate results so these incremental sizes were chosen for comparison (Chang and wen 2007). The Fig. 9 shows the time-history displacement of the bridge deck in the longitudinal direction under near-field earthquake of Irpinia (20 sec) and it can be inferred that the behavior of the model for both increment sizes is similar (almost). The maximum relative displacements are illustrated in the Table 4. As the increment size changes from 0.001 to 0.0001, the maximum relative displacement increases around 0.4%. Therefore, the increment size of 0.001 is suitable in this case study.

4.3.2 Mesh optimization

Several factors affect the selection of kind of mesh and its size, such as the type and method of analysis, model features, model geometry and so on. On the other hand, the type and size of the mesh directly affect the results and time of analysis. In order to achieve the best size of the mesh, the value of the fundamental period of the target bridge is conducted with different sizes of mesh which is shown in Fig. 10. The eigenvalue analysis is based on AMS eigen-solver.

Obviously, the lowest frequency of vibration is the natural or fundamental frequency of vibration of the system. For an RC bridge with 2 to 4 lines, spans length of 10-95 m, column length of 5-30 m and the deck of composite steel and concrete (like the bridge model of this study) the empirical estimated natural frequency will be in the range of 0.5-2.5 Hz or 2-0.4 sec (Maia *et al*. 1997). The fundamental frequency of the studied bridge has been calculated equal to 1.32 Hz (0.75 sec) which is in the range of the above. The best size of mesh (the biggest one with the accurate answer) is chosen (Table 5). The kind of mesh which is considered for this analysis is 8-node linear brick

(deck and steel beams), 6-node linear triangle (columns) and 2-node linear 3-D truss (rebars).

According to the Table 5, the mesh size corresponds to 7900 mesh will be the best choice and considered for analysis.

4.4 Ground motion records

4.4.1 Near-field and far-field acceleration records

In this study, the definition for selecting near-field ground motion records is the records with less than 15 km of Joyner-Boor distance (defined as the closest horizontal distance to the surface projection of the fault plane. R-JB≤15 km) and ground motions with more than 20 km of R-JB have a far-field effect (Lin *et al*. 2013). In order to study the behavior of structure more accurate under near-field and far-field records, 3 earthquake events in two vertical and horizontal components have been chosen from the PEER ground motion database and have been illustrated in Table 6 (PEER database). The acceleration records have been shown in Figs. 11-13. The near-field and far-field records have been chosen pairwise from the same events which are fits to the seismic design of the bridge. This kind of selection will help to compare the results more meaningful. It is notable that the current analysis is conducted based on this assumption that the bridge is located on a rigid surface and the type of site soil and acceleration records match with the bridge seismic design assumptions.

4.4.2 Response acceleration spectra of records

Table 7 shows the response acceleration spectra of the ground motion records at the period of 0.75 sec which corresponds to the fundamental period of the bridge model in the longitudinal direction (see section 4.3.2).

For near-field ground motions, Irpinia has the highest response acceleration (21.63 m/s^2 for the period of 0.75 sec) and for the far-field ground motions Chi-Chi has the highest response acceleration, equal to 16.14 m/s^2 at the fundamental period of the bridge. The diagrams of response
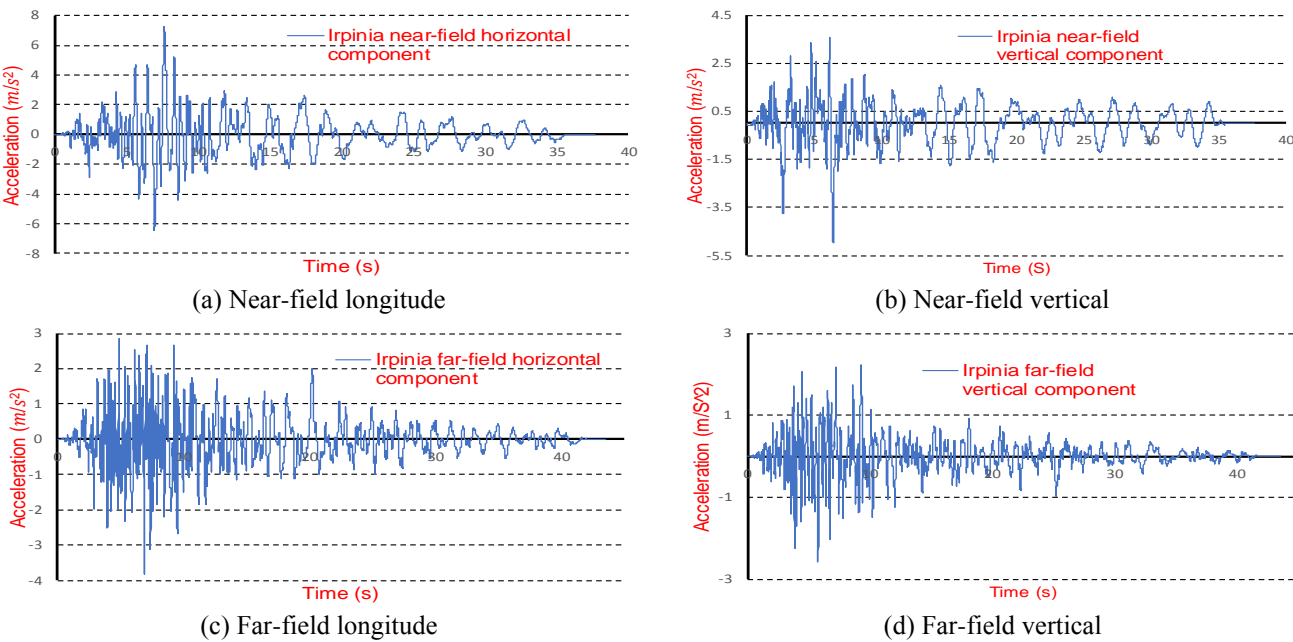
(a) Near-field longitude

(b) Near-field vertical

(c) Far-field longitude

(d) Far-field vertical

Fig. 11 Acceleration records of Irpinia ground motion

(a) Near-field longitude

(b) Near-field vertical

(c) Far-field longitude
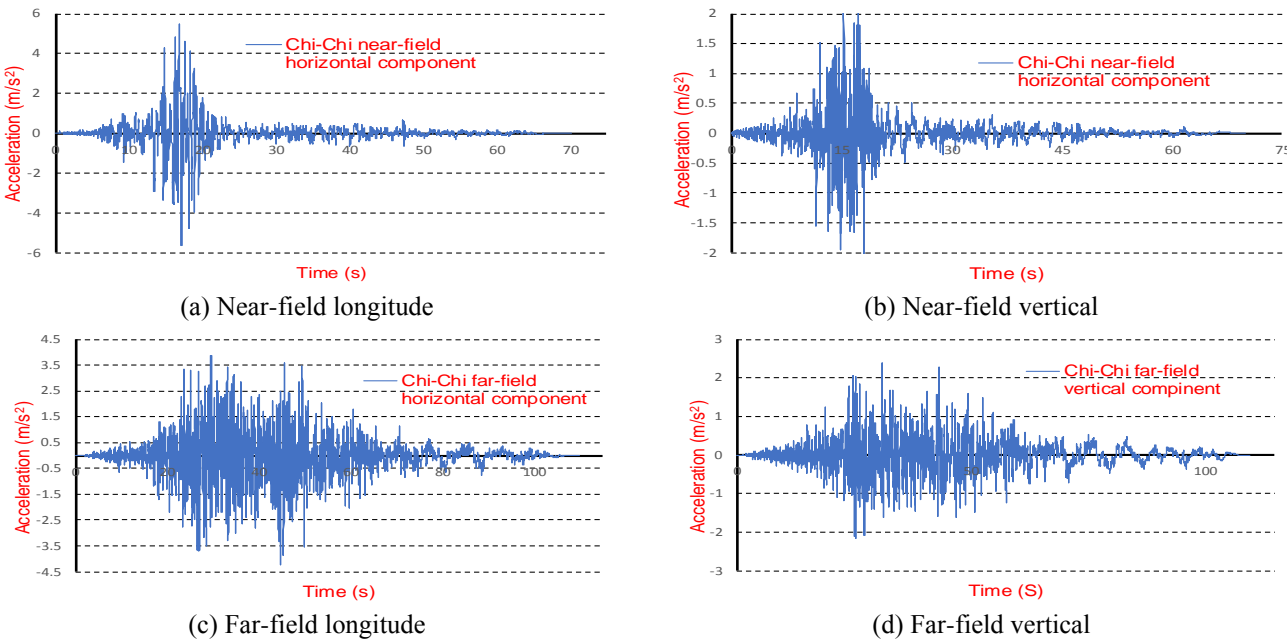

(d) Far-field vertical

Fig. 12 Acceleration records of Chi-Chi ground motion

Table 6 Acceleration records of near-field and far-field ground motions

Near-field acceleration records					Far-field acceleration records				
Event	Component	PGA ($\frac{m}{s^2}$)	Magnitude (R)	R-JB (km)	Event	Component	PGA ($\frac{m}{s^2}$)	Magnitude (R)	R-JB (km)
Manjil	Longitude	5.23	7.37	12.55	Manjil	Longitude	2.04	7.37	174.55
	Vertical	5.19				Vertical	1.27		
Chi-Chi	Longitude	6.08	7.62	3.12	Chi-Chi	Longitude	4.42	7.62	63.21
	Vertical	2.13				Vertical	2.38		
Irpinia	Longitude	7.16	6.20	4.73	Irpinia	Longitude	3.89	6.20	41.73
	Vertical	3.97				Vertical	2.57		

acceleration spectra for ground motion records have been shown in Fig. 14.

As shown in Fig. 14 In near-field records the Chai-Chai ground motion has the highest response acceleration 23.23
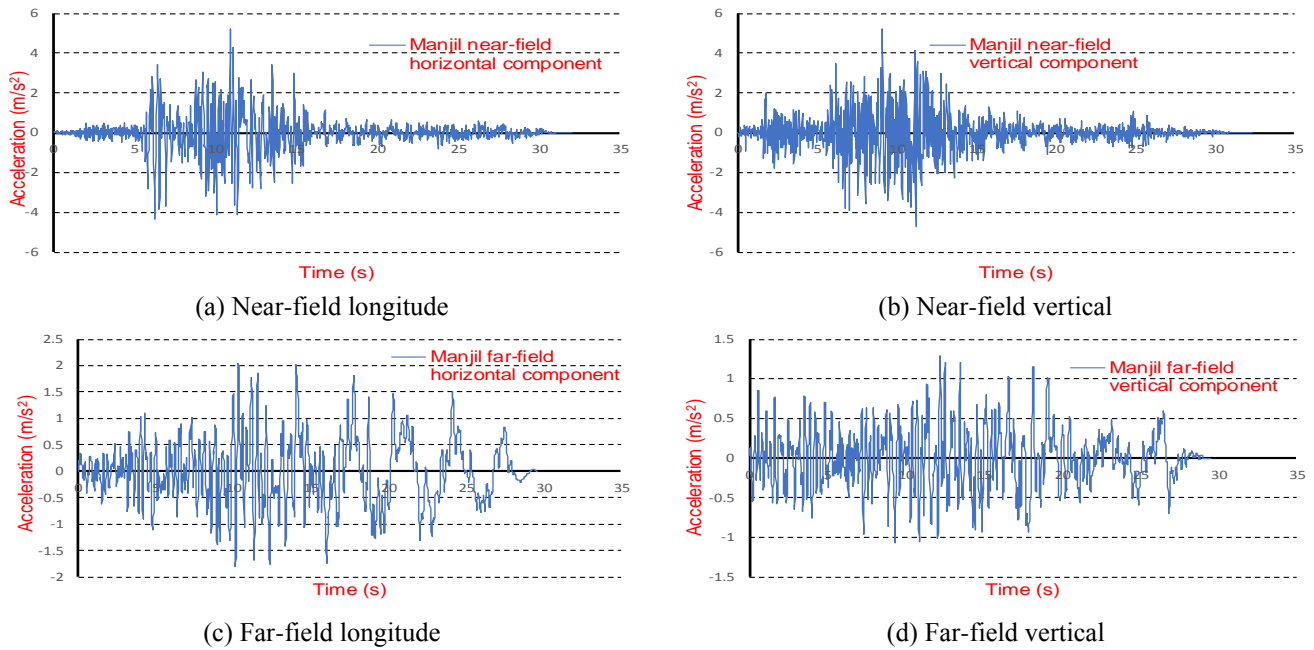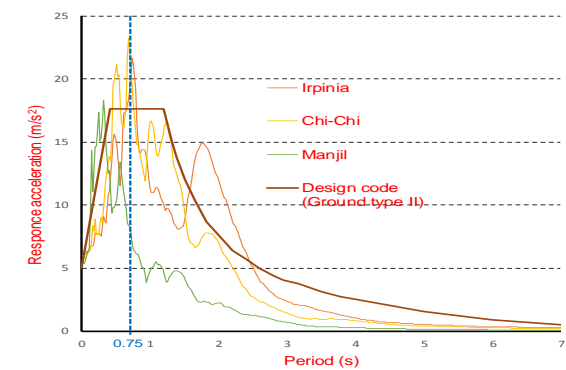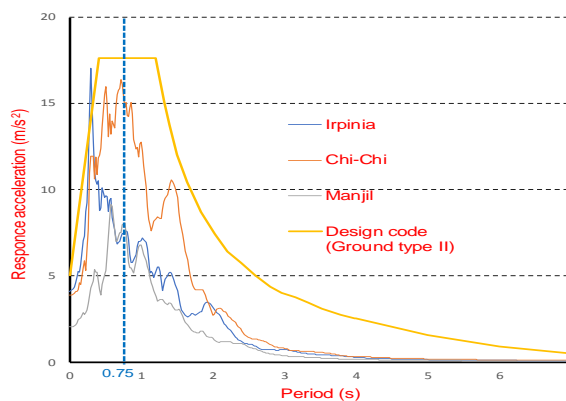
(a) Near-field longitude

(b) Near-field vertical

(c) Far-field longitude

(d) Far-field vertical

Fig. 13 Acceleration records of Manjil ground motion

Table 7 Maximum response acceleration corresponding to the period of 0.75 sec.

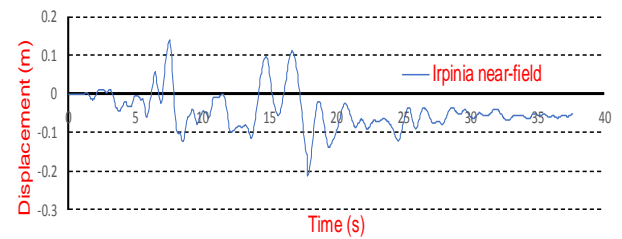| Event	Near-field ($\frac{m}{s^2}$)	Far-field ($\frac{m}{s^2}$)
Irpinia	21.63	7.47
Chi-Chi	19.63	16.14
Manjil	7.56	7.02

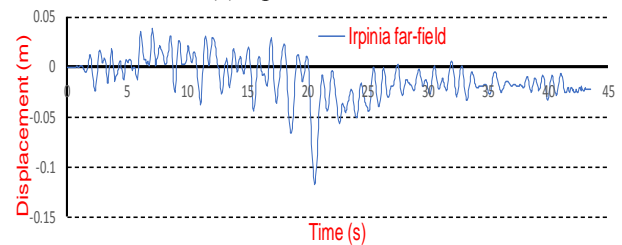(a) Near-field longitude

(b) Far-field longitude

Fig. 14 Response acceleration spectra of ground motions

(a) Irpinia near-field

(b) Irpinia far-field

Fig. 15 Longitude deck displacement time history

m/s^2 at the period of 0.68sec and in case of far-field records, the Irpinia ground motion has the highest response acceleration, equal to 17.04 m/s^2 in 0.3sec.

5. Results of seismic behavior of the bridge model

5.1 Relative displacement response

The time histories of relative displacement of the deck of the bridge are presented in Figs. 15-17. The acceleration records hit the bridge in two components of vertical and longitude. Note that by studying the mode shapes and related frequencies, the response displacements are generally larger in the longitudinal direction than the transverse direction and this is why two components of
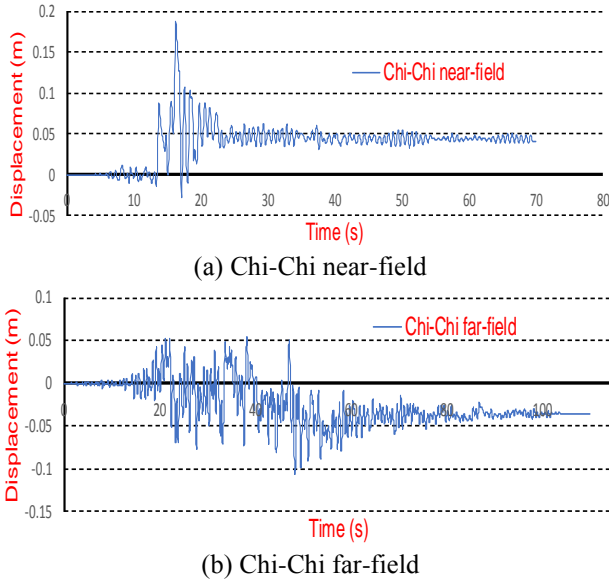
(a) Chi-Chi near-field

(b) Chi-Chi far-field

Fig. 16 Longitude deck displacement time history
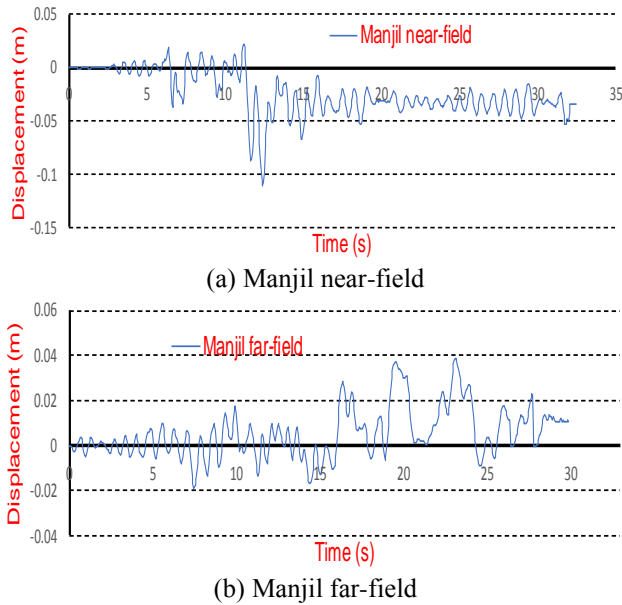

(a) Manjil near-field

(b) Manjil far-field

Fig. 17 Longitude deck displacement time history

Table 8 Maximum relative displacement of the deck

Event	Near-field (m)	Far-field (m)
Irpinia	0.21	0.11
Chi-Chi	0.18	0.10
Manjil	0.11	0.04

Table 9 Maximum longitude residual displacement

Event	Near-field (m)	Far-field (m)
Irpinia	0.057	0.022
Chi-Chi	0.042	0.035
Manjil	0.033	0.011

Table 10 Maximum plastic strain

Event	Near-field (m)	Far-field (m)
Irpinia	1.607e-1	6.785e-2
Chi-Chi	1.428e-1	1.032e-1
Manjil	9.059e-2	3.895e-2

(a) Irpinia ground motion

(b) Chi-Chi ground motion

(c) Manjil ground motion
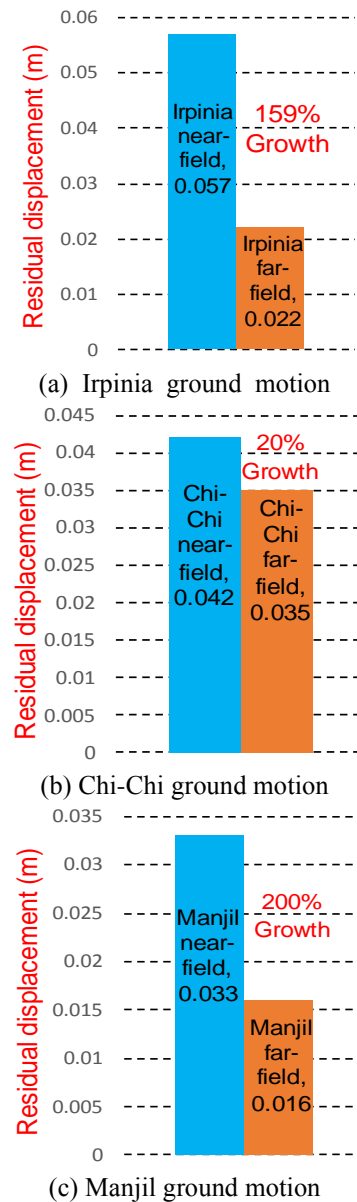
Fig. 18 Growth of longitude maximum residual displacement

vertical and longitude have been selected. The relative displacements are in the range of 0.21 to 0.04 m.

In all cases, the values of relative displacements relevant to near-field ground motions are bigger than related far-field ground motion. As it has been shown in Table 8 the relative displacement of near-field Irpinia shows 90% (almost twice) growth in comparison to far-field ground motion. Also, the maximum relative displacement of near-field Chi-Chi and Manjil shows respectively 80% and 175% of growth. As it is presented, the near-field ground motions can cause even more than triple of relative displacement in structures in comparison with the related near-field ground motion which in some cases, can cause serious damage and collapse.
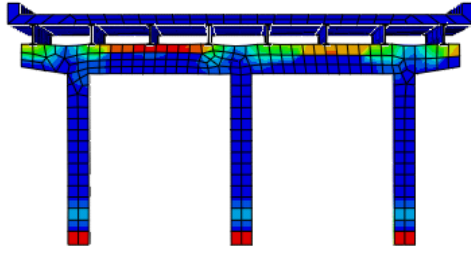
Fig. 19 Place of plastic strain in transverse section

(a) Kelvin-Voight

(b) FVD-B-1000-1200

Fig. 20 Damper model

5.2 Residual displacement

This section presents the residual displacement and plastic strain of the bridge model in both near-field and far-field cases. Ground motions from section 4.4 cause permanent or residual displacement which is clear in Figs. 15-17. This amount depends on factors such as mass, stiffness, fundamental period, the frequency content of acceleration record and so on (Kawashima *et al.* 1998). The residual displacement can be taking account as an undesirable indicator that shows damage and failure in the structure which affects the performance of the structure. Table 9 and Fig. 18 show that the longitude residual displacement has grown under near-field ground motions in comparison with far-field ground motions, in all cases. The Manjil near-field shows 200% of growth in residual displacement which is the highest amount of growth, this value is 20% and 159% for Chi-Chi and Irpinia ground motions respectively. This amount (growth of residual displacement) can change and affect all the expected damage, performance, repair process, costs and behavior of the structure. Also, the value of plastic strain shows the same behavior under near-field and far-field ground motions. Fig. 19 and Table 10 show the value and the place of plastic strain.

5.3 Seismic control

Based on the bridge design code (Nihon Doro *et al.* 1998). Residual displacement of the bridge model needs to be checked for Type B bridges under seismic load (see section 2). The maximum residual displacement should satisfy the value of the design code which is presented by Eq. (8)

$$d_R \leqslant d_{R-allowable} \qquad (8)$$

where:

d_R: The maximum residual displacement of the bridge column

$d_{R-allowable}$: The allowable residual displacement which presented by design code. it is 1 present of the height of the bridge column which has been calculated by Eq. (9).

$$d_{R-allowable} = 0.01 \times 7.315\text{m} = 0.073\text{m} \qquad (9)$$

Based on Table 9 the maximum residual displacement of the bridge deck is $d_R = 0.057$ m which relates to Irpinia near-field ground motion. Note that this value presents a more critical residual displacement condition than the
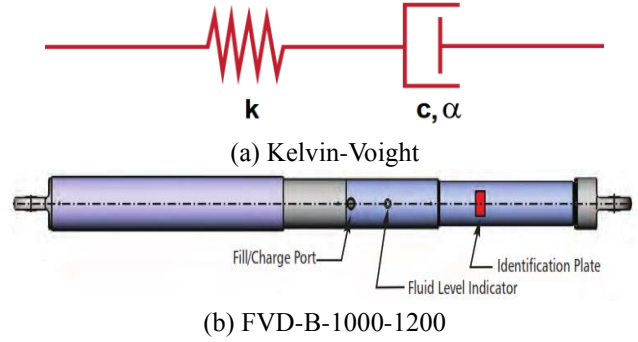

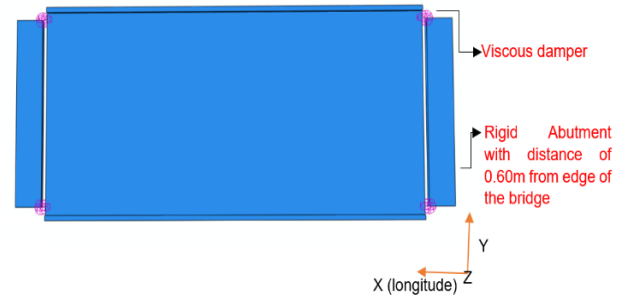Fig. 21 Plan of the bridge model with four viscous dampers

Table 11 Viscous damper details

Catalog No./Model	Damping coefficient (kN/m/sec)$^\alpha$	α	Stroke size (m)	Unit weight (kg)
FVD-B-1000-1200	1000	1	0.60	735

*α: The velocity exponent (0.2≤α≤1) which is considered 1 (linear) in this study.

column. As it is clear in Eq. (10), the design code criteria ($d_R \leqslant d_{R-allowable}$) satisfied in all near-field and far-field ground motion cases.

$$0.057m \leqslant 0.073m \quad \checkmark\text{OK} \qquad (10)$$

5.4 Bridge model with viscous damper

As it was mentioned (section 5.1 and 5.2) in all 3 groups of ground motions the model shows different seismic behavior under near-field and far-field ground motions. The parameters of relative and residual displacement grow under near-field ground motions in comparison with the far-field. This different seismic behavior has not been considered in seismic design codes directly. Therefore, in order to decrease the undesirable effect of near-field ground motions a plan based on the viscous damper is suggested in this study. This suggestion is based on a fluid viscous damper of FVD-B Series (ITT Enidine Inc. 2019). The details of the viscous damper have been illustrated in Fig. 20 and Table 11.

Viscoelastic dampers can be modeled by a combination of springs and ideal viscous dampers. As it is shown in Fig. 20(a) the Kelvin-Voight model (a spring and a viscous damper in parallel) is used to model the Viscous damper in this study (Meyers and Chawla 1999).

Table 12 Longitude time-history displacement of models under Chi-Chi ground motion

Event/Model type	Maximum relative displacement (m)	Maximum residual displacement (m)
Chi-Chi near-field/ without damper	0.180	0.042
Chi-Chi far-field/ without damper	0.101	0.035
Chi-Chi near-field/ with damper	0.078	0.015

Fig. 23 Longitude displacement time history of the model with and without viscous dampers under Chi-Chi near field ground motion
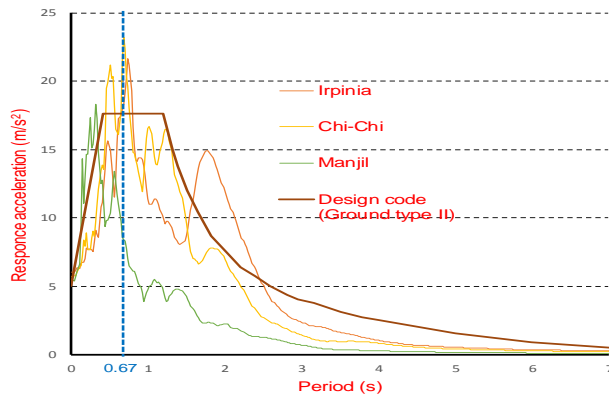

Fig. 22 Near-field response acceleration spectra of ground motions

Four number of viscous dampers have been used to connect the first and the last steel beams to the abutment. The places of viscous dampers have been shown in Fig. 21. The abutment is assumed as rigid.

The dampers increase the frequency of the first mode of the structure from 1.33 Hz to 1.48 Hz (11% increase in frequency) so the fundamental period of the structure has been changed from 0.75 sec to 0.67 sec. Corresponding to Fig. 22 and the period of 0.67, the Chi-Chi near-field ground motion has the highest value of response acceleration (23.23 m/s²) in comparison with other ground motions from section 4.4.1.

By comparing the longitude displacement time-history of the bridge with and without dampers under Chi-Chi ground motion which is illustrated in Fig. 23, the maximum relative and residual displacement decrease 56% and 64% respectively. These values (model with the damper) are even less than the maximum relative and residual displacement of the bridge model under Chi-Chi far-field ground motion, around 22%, and 57% respectively fewer. These values have been presented in Table 12.

6. Conclusions

To evaluate the seismic behavior of bridge model under near-field and far-field ground motions, an RC bridge model with a span length of 21.87 m, total deck length of 43.74 m and column height of 7.315 m were numerically studied under horizontal and vertical components of near-field and far-field ground motions. The parameters of relative displacement, residual displacement, and plastic
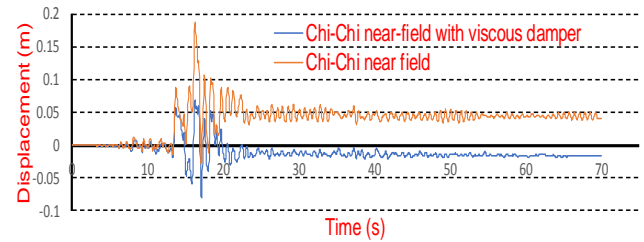
strain have been compared. Finally, to decrease the undesirable effect of near-field ground motions on the model, a plan based on viscous dampers is suggested and its results were compared with and without damper model. The evaluations indicate that:
• By comparing the value of PGA and response acceleration spectra (for the period of less than 4sec) in all components of horizontal and vertical of near-field acceleration records, it is observed that these parameters are higher than related far-field ground motions. This could be one of the main reasons that the near-field ground motions are more destructive in this study.
• The study of maximum relative displacements shows that this parameter in near-field ground motions is significantly more than related far-field ground motions, even more than three times. This parameter shows 90%, 80% and 175% of growth respectively under Irpinia, Chi-Chi and Manjil earthquakes.
• The value of residual displacement has grown dramatically in terms of near-field ground motions. These values of growth for Irpinia, Chi-Chi, and Manjil ground motions are 159%, 20%, and 200% respectively. The value of plastic strain also shows the same behavior.
• The viscous dampers are useful and improve the seismic behavior of the bridge model even under near-field ground motions a lot. The bridge model with viscous damper under near-field ground motion shows fewer relative and residual displacement, even fewer than related far-field ground motion. For relative displacement, under Chi-Chi near-field earthquake use of viscous damper decreases 56% and 22% respectively in comparison with near-field and far-field ground motions.

References

Abaqus Tutorial (2010), Version 10.1 Getting Started with ABAQUS Interactive Edition.
Bertero, V.V., Mahin, S.A. and Herrera, R.A. (1978), "Aseismic design implications of near-fault San Fernando earthquake records", *Earthq. Eng. Struct. Dyn.*, **6**(1), 31-42. https://doi.org/10.1002/eqe.4290060105.
Bolt, B.A. (1993), *Earthquakes*, WH Freeman and Company,San Francisco.
Chang, S.Y. and Liao, W.I. (2005), "An unconditionally stable explicit method for structural dynamics", *J. Earthq. Eng.*, **9**(3), 349-370.
Cook, R.D. (2007), *Concepts and Applications of Finite Element*

Analysis, John Wiley & Sons.

Corigliano, M. (2007), "Seismic response of deep tunnels in near-fault conditions", Politecnico di Torino, Italy.

Davoodi, M. and Sadjadi, M. (2015), "Assessment of near-field and far-field strong ground motion effects on soil-structure SDOF system", *Int. J. Civil Eng.*, **13**(3), 153-166.

Davoodi, M., Sadjadi, M., Goljahani, P. and Kamalian, M. (2012), "Effects of near-field and far-field earthquakes on seismic response of sdof system considering soil structure interaction", *15th World Conference on Earthquake Engineering*, Lisbon, Portugal.

Hibbitt, H.D. and Karlsson, B.I. (1979), "Analysis of pipe whip (No. EPRI-NP--1208)", Hibbitt and Karlsson.

Hilber, H.M., Hughes, T.J. and Taylor, R.L. (1977), "Improved numerical dissipation for time integration algorithms in structural dynamics", *Earthq. Eng. Struct. Dyn.*, **5**(3), 283-292. https://doi.org/10.1002/eqe.4290050306.

Hoshikuma, J.I., Zhang, G. and Sakai, J. (2011), "Seismic behavior of retrofitted bridges during the 2011 great east Japan earthquake", *Proceedings of the International Symposium on Engineering Lessons Learned from the 2011 Great East Japan Earthquake*, Tokyo, Japan, March.

Hsu, L.S. and Hsu, C.T. (1994), "Complete stress-strain behaviour of high-strength concrete under compression", *Mag. Concrete Res.*, **46**(169), 301-312. https://doi.org/10.1680/macr.1994.46.169.301.

ITT Enidine Inc. (2019), Infrastructure Products, Orchard Park, New York, USA.

Kawashima, K., MacRae, G.A., Hoshikuma, J.I. and Nagaya, K. (1998), "Residual displacement response spectrum", *J. Struct. Eng.*, **124**(5), 523-530. https://doi.org/10.1061/(ASCE)0733-9445(1998)124:5(523).

Lin, L., Ruizhi, W., Baofeng, Z. and Dacheng, S. (2013), "The selection and scaling of ground motion records for great scenario earthquakes based on the condition mean spectrum", *Acta Seismologica Sinica*, **35**(3), 380-389.

Maia, N.M.M., Silva, J.M.M. and He, J. (1997), *Theoretical and Experimental Modal Analysis*, Research Studies Press, Taunton, England.

Meyers, M.A. and Chawla, K.K. (2008), *Mechanical Behavior of Materials*, Cambridge University Press.

Mohammadi, M.H., Massumi, A. and Meshkat-Dini, A. (2017), "Performance of RC moment frames with fixed and hinged supports under near-fault ground motions", *Earthq. Struct.*, **13**(1), 89-101. https://doi.org/10.12989/eas.2017.13.1.089.

Mohammadi, M.H., Massumi, A. and Meshkat-Dini, A. (2019), "Near-fault effects on the seismic demand of RC buildings in linear and nonlinear analyses", *Scientia Iranica*, **26**(1), 188-201.

Nihon Doro, K. (2002), "Design specifications for highway bridges", Japan Road Association, Tokyo.

Nihon Dōro, K., Unjoh, S., Terayama, T. and Doboku, K. (1998), "Design specifications for highway bridges: Part 5. Tsukuba-shi: The division".

PEER Ground Motion Database. Available from University of California, Berkeley PEER Ground Motion, from University of California, Berkeley, https://ngawest2.berkeley.edu/.

Ramberg, W. and Osgood, W.R. (1943), "Description of stress-strain curves by three parameters", NACA Technical Note 902, 1-29.

Sheikh, M.N., Legeron, F. and Tsang, H.H. (2012), Seismic Performance of Bridges Designed According to AS 5100.

Somerville, P.G., Smith, N.F., Graves, R.W. and Abrahamson, N.A. (1997), "Modification of empirical strong ground motion attenuation relations to include the amplitude and duration effects of rupture directivity", *Seismol. Res. Lett.*, **68**(1), 199-222. https://doi.org/10.1785/gssrl.68.1.199.

Stewart, J.P., Chiou, S.J., Bray, J.D., Graves, R.W., Somerville, P.G. and Abrahamson, N.A. (2002), "Ground motion evaluation procedures for performance-based design", *Soil Dyn. Earthq. Eng.*, **22**(9-12), 765-772. https://doi.org/10.1016/S0267-7261(02)00097-0.

Zhang, Q., Gong, J.X. and Zhang, Y.Q. (2013), "Lateral-load behavior prediction and pushover analysis of reinforced concrete columns including shear effects", *Adv. Struct. Eng.*, **16**(4), 741-758. https://doi.org/10.1260/1369-4332.16.4.741.

CC